

Comparative study on interatomic force constants and elastic properties of zinc-blende AlN, AlP and AlAs

H. Wang¹⁾, Q. Tan, X. Zeng

Department of Physics and Electronic Information Engineering, Xiangnan University,
423000 Chenzhou, The People's Republic of China

Submitted 25 February 2019

Resubmitted 25 February 2019

Accepted 21 March 2019

DOI: 10.1134/S0370274X19100060

Almost all epitaxial AlN, AlP and AlAs films are expected to contain some residual strain. A knowledge of their elastic constants and strain deformation potentials is indispensable. Although there are many theoretical [1–3] and experimental [4, 5] results, there is a lack of systematic research on their elastic constants and behaviors under hydrostatic and uniaxial stress. The purpose of this study is to study the above properties of these compounds by pseudopotential method, and the linear response by density functional theory (DFT) and density functional perturbation theory (DFPT). The norm-conserving non-local Troulliers–Martins pseudopotentials [6] is employed. The Kohn–Sham orbits are expanded in plane waves basis set. The Troullier and Martins programs generate soft core pseudopotential. The theoretical calculation is performed by using the local density approximation of the exchange–correlation Hamiltonian as implemented in abinit package [7].

In this calculation, Al ($3s^23p^1$), N ($2s^22p^3$), P ($3s^23p^3$), and As ($4s^24p^3$) shells are used as valence band electrons. The ground state equilibrium volumes of zinc-blende AlN, AlP and AlAs are determined by calculating the total energy of each primitive unit cell as a function of V . The calculated energy volume data are fitted with Monahan's equation of state. The obtained structural parameters are 4.352 Å, 5.442 Å and 5.613 Å respectively.

The interatomic force constants (IFC) describing the atomic interactions in a crystalline solid are defined in real space as [8]:

$$C_{k\alpha, k'\beta}(a, b) = \frac{\partial^2 E}{\partial \tau_{k\alpha}^a \partial \tau_{k'\beta}^b} = C_{k\alpha, k'\beta}^{\text{ion}}(a, b) + C_{k\alpha, k'\beta}^{\text{elec}}(a, b). \quad (1)$$

Here, $\tau_{k\alpha}^a$ is the displacement vector of k -th atom in the a -th primitive cell along α axis. E is the Born–

Oppenheimer (BO) total energy surface of the system (electrons plus clamped ions) where C^{ion} and C^{elec} are the ionic contribution and electronic contribution to the force constants, respectively for other variables, see [8]. For this reason, IFC offer a convenient way of storing the information contained in the dynamical matrix at any q into a few independent parameters. Therefore, it is necessary to fully describe the ion motion in DFPT. Fourier analysis is used to calculate and tabulate a set of force constant matrices on uniform meshes in reciprocal space. Real space force constants can be easily obtained:

$$C_{k\alpha, k'\beta}(\mathbf{R}) = \frac{1}{N} \sum_q e^{i\mathbf{q}\mathbf{R}} \tilde{C}_{k\alpha, k'\beta}(\mathbf{q}), \quad (2)$$

Here N is the number of unit cells in the crystal. After calculating the real space constants by this method, the reciprocal-space dynamic matrix can be obtained by inverse Fourier transform at any q point of Brillouin region.

The dynamical matrices have been calculated on a ($8 \times 8 \times 8$) reciprocal space face centered cubic (FCC) grid. Fourier deconvolution on its mesh yields real-space interatomic force constants up to the ninth neighbor shell. This process is equivalent to calculate real space force constant using the FCC supercell, which linear size is four times that of the primitive zinc-blende cell, so it contains 128 atoms.

As seen from Fig. 1, in general, the decay of local interaction for cation-cation, cation-anion, and anion-anion is faster than the total interaction decay. In the fourth neighbor, the local part of each species pair tends to zero, while the total part of cation-cation, cation-anion and anion-anion interaction of AlAs tends to zero only in the eighth neighbor, and the rest in the ninth neighbor has not yet tended to zero.

The elastic constants of solids provide interesting information about their mechanical and dynamic properties and provide a link between the dynamics and mechanical behavior of crystals. The calculated elastic con-

¹⁾e-mail: whycs@163.com

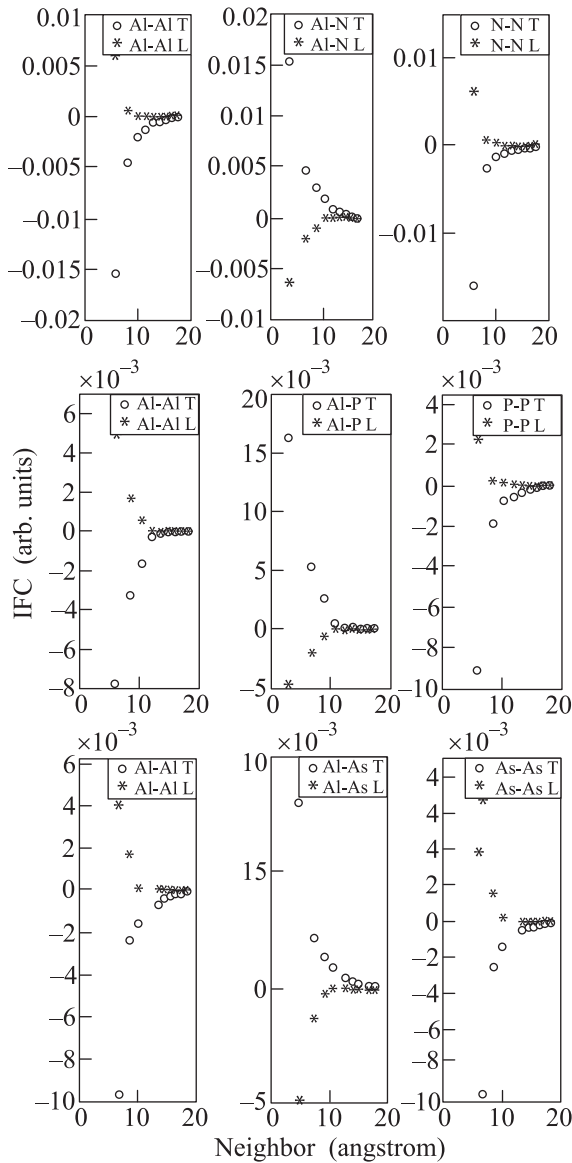


Fig. 1. The upper, middle, and lower figures, respectively, show the IFC for zinc-blende AlN, AlP and AlAs. From left to right, show the behavior of the total IFC (“T” represent total) and of the local contribution (“L” represent local) as a function of interneighbour distance for cation-cation, cation-anion and anion-anion interaction

stants C_{11} , C_{12} and C_{44} are 318, 171 and 182 (in GPa) for AlN, 133.6, 67.2 and 78.6 (in GPa) for AlP, 125.5, 62.4 and 63.2 (in GPa) for AlAs, respectively.

Comparing the elastic constants of AlN, AlP and AlAs calculated in this paper, the elastic constants of AlN are obviously higher than those of the other two values, but the difference between AlP and AlAs is not significant. The reason is that the lattice constants of the compounds increase with the increase of the number of anion atoms, while the difference of electroneg-

ativity between anions and cations decreases, and the binding force between ions and ions decreases, which result in elastic constants of the compounds decrease in turn. Moreover, the lattice constants of AlN are obviously smaller than those of AlP and AlAs, but the lattice constants of AlP and AlAs are almost the same, furthermore, the difference of internal nuclear charge is not taken into account in the selection of P and As pseudopotentials, and the distribution of valence charge density is not very different, so the elastic constants of AlN are obviously higher than those of AlP and AlAs, and the latter two values are not very different.

In order to better illustrate the elastic behavior of these crystals, we schematically drew the young’s modulus surface of these materials. Although the zinc-blende structure has high symmetry, the elastic behavior of the whole crystal cannot be represented by a single surface. Following formula [9], Young’s modulus of three compound semiconductors (101) is calculated.

$$E = \frac{1}{C_{11}} - 2 \left(\frac{1}{C_{11}} - \frac{1}{C_{12}} - \frac{1}{C_{44}} \right) (l_1^2 l_2^2 + l_2^2 l_3^2 + l_3^2 l_1^2). \quad (3)$$

Here, l_1 , l_2 and l_3 are cosines of azimuth. Young’s moduli are not isotropic in the cubic system. The variation with direction depends on $(l_1^2 l_2^2 + l_2^2 l_3^2 + l_3^2 l_1^2)$, and the quantity is zero in $\langle 100 \rangle$ direction but has a maximum value $1/3$ in the $\langle 111 \rangle$ direction. The sagittal diameter is directly proportional to the surface of Young’s modulus, and it is a circular cube in the central depression of each surface.

Full text of the paper is published in JETP Letters journal. DOI: 10.1134/S0021364019100035

1. A. A. Yamaguchi, Y. Mochizuki, C. Sasaoka, A. Kimura, M. Nido, and A. Usui, *Appl. Phys. Lett.* **71**, 374 (1997).
2. Y. Ciftci, K. Colakoglu, and E. Deligoz, *Phys. Stat. Sol. (c)* **4**, 234 (2007).
3. A. F. Wright, *J. Appl. Phys.* **82**, 2833 (1997).
4. I. Petrov, E. Mojab, R. C. Powell, J. E. Green, L. Hultman, and J. E. Sundgren, *Appl. Phys. Lett.* **60**, 2491 (1992).
5. G. Lucovsky, R. M. Martin, and E. Burstein, *Phys. Rev. B* **4**, 1367 (1971).
6. N. Troullier and J. L. Martins, *Phys. Rev. B* **43**, 1993 (1991).
7. X. Gonze, J. M. Beuken, R. Caracas et al. (Collaboration), *Comput. Mater. Sci.* **25**, 478 (2002).
8. P. Giannozzi and S. de Gironcoli, *Phys. Rev. B* **43**, 7231 (1990).
9. J. F. Nye, *Physical Properties of Crystals, Their Representation by Tensors and Matrices*, 2-nd ed., Oxford, Clarendon (1985).